# Inelastic Tunneling Spectroscopy of Alkanethiol Molecules: High-Resolution Spectroscopy and Theoretical Simulations

Norio Okabayashi,[1,2] Magnus Paulsson,[3,4] Hiromu Ueba,[4] Youhei Konda,[1] and Tadahiro Komeda[1,2,*]
[1] *Institute of Multidisciplinary Research for Advanced Materials (IMRAM), Tohoku University, Sendai, 980-8577, Japan*
[2] *CREST, Japan Science and Technology Agency (JST), Saitama 332-0012, Japan*
[3] *School of Computer Science, Physis and Mathematis, Linnaeus University, 391 82 Kalmar, Sweden*
[4] *Department of Electronics, University of Toyama, Toyama, 930-8555, Japan*
(Received 25 September 2009; published 18 February 2010)

We investigate inelastic electron tunneling spectroscopy (IETS) for alkanethiol self-assembled monolayers (SAM) with a scanning tunneling microscope and compare it to first-principles calculations. Using a combination of partial deuteration of the molecule and high-resolution measurements, we identify and differentiate between methyl ($CH_3$) and methylene ($CH_2$) groups and their symmetric and asymmetric C-H stretch modes. The calculations agree quantitatively with the measured IETS in producing the weight of the symmetric and asymmetric C-H stretch modes while the methylene stretch mode is largely underestimated. We further show that inelastic intermolecular scattering is important in the SAM by plotting the theoretical current densities.

DOI: 10.1103/PhysRevLett.104.077801 PACS numbers: 73.61.Ph, 68.37.Ef, 72.10.−d, 73.50.−h

Electron transport through molecular wires has been intensively studied during the past decade [1]. This interest has been fueled by the vision of molecular electronics and will in addition improve our understanding of electron transport at the nanoscale. Inelastic electron tunneling spectroscopy (IETS) measures the change in conductance as electrons excite vibrations and is an important tool to characterize molecules in metallic junctions [2]. It can help both in the determination of the actual chemical species and to increase our understanding of the transport mechanism. Alkanethiols contacted by gold electrodes [$CH_3$-$(CH_2)_n$-S-Au] has been widely used as a standard molecule in these studies, and the IETS has been measured using several different contacting strategies, e.g., scanning tunneling microscope (STM) [3], crossed wire junctions [4], and nanopore junctions [5]. The IETS shows several vibration modes in the energy range of the C-C stretching [$\nu$(C-C)] and CH bending modes as well as the C-H stretch [$\nu$(C-H)] region.

In contrast to infrared (IR) and Raman spectroscopy, there is a lack of systematic experimental investigations of the selection rules for the IETS. To our knowledge, the only experimental work towards a quantitative understanding of the IETS scattering cross section is the work by Beebe *et al.*, in which alkanemonothiol molecules were systematically fluorinated from the methyl end ($CH_3$ group furthest away from the Au-S bond) [6]. They observed that the intensity of the $\nu$(C-H) mode was insensitive to the partial fluorination and concluded that the dominant contribution of the $\nu$(C-H) mode is from the sulfur-metal contact region (linker part) rather than the methyl group. In addition, theoretical methods have made tremendous progress in the analysis of the IETS [7–12]. Nonequilibrium Green's function methods combined with density functional theory (DFT) agree at least qualitatively with the $\nu$(C-C), C-H bending and $\nu$(C-S) modes [7–12]. However, the $\nu$(C-H) mode, which has been observed to have one of the largest signals in experiments, is in general much smaller in calculations.

In this Letter we examine the IETS of the $\nu$(C-H) mode for alkanethiol self-assembled monolayers (SAM) using STM measurements and first-principles calculations. By deuteration of the terminal methyl group [$CH_3$-] we successfully detected and classified the site-dependent peak positions of the vibrational modes from high-resolution IETS. Especially for the methyl group, the asymmetric $\nu$(C-H) mode gives a larger signal than the symmetric mode. The theoretical simulations reproduce the $CH_3$ stretch mode IETS intensities but fail to quantitatively describe the $CH_2$ stretch modes. These results allow us to critically compare the theory to the measurements, and to discuss the IETS selection rules together with tunneling pathways through the SAM.

Details of the experimental method have been described in our previous paper [13], and we only briefly comment on the current setup. The methyl group deuterated alkanethiol molecule $CD_3(CH_2)_7SH$, hereafter called $CD_3$-$C_7$, were synthesized from commercially available $CD_3(CH_2)_7Br$ (CDN isotopes, Canada) [14]. SAM of the deuterated and normal hydrogen alkanethiol ($CH_3$-$C_7$) were prepared by adsorption of molecules from a solution. Cryogenic STM was used to confirm the well-known $\sqrt{3} \times \sqrt{3}R30°$ structure of SAM on Au(111) [3]. After the tip was laterally set to the bright spot of the topographic image, the tip was moved closer to the surface (1 nA at 0.5 V) in order to improve the signal-to-noise ratio. Note that the tip actually pushes the SAM since the tip is approximately 1.5 Å closer than the contact point [3]. Thereafter, the IETS was measured by the standard method [13] with lock-in amplifiers at 4.4 K.

The theoretical calculations were performed with previously reported methods [11,12,15,16]. Using the SIESTA [17–19] DFT code, the geometry of the $\sqrt{3} \times \sqrt{3}R30°$ structure of octanethiol, bound to a Au(111) slab, was relaxed. This geometry was thereafter repeated to give a unit cell containing four molecules ($2 \times 2$), and the STM tip was simulated with one Au atom protruding from the Au(111) slab (smallest tip-C distance 3.3 Å). Since we utilized periodic boundary conditions and model both tip and substrate using the same Au(111) slab, the tip atom was displaced by 1.2 Å, along the surface, from the center of the $CH_3$ end group of one molecule. The IETS was calculated using the lowest order expansion (LOE) method by combining the electron-phonon ($e$-ph) coupling with the elastic electron transport properties calculated using the nonequilibrium Green's function program TRANSIESTA [20]. Broadening by lock-in voltage and temperature were included. Note that the LOE assumes (i) weak $e$-ph coupling and (ii) a slowly varying density of states around the Fermi energy. These approximations are well justified for alkanethiol on Au(111) since (i) less than 3% of the electrons undergo inelastic scattering [3] and (ii) the conductance is almost bias independent [3].

The measured and calculated IETS for the $CH_3$-$C_7$ SAM are shown in Fig. 1. The vertical axis of $d^2I/dV^2$ was normalized by the $dI/dV$ to cancel effects of the tip-substrate distance [21]. This allows us to compare the experimental IETS taken at a low bias conductance of 2 nA/V with the calculations performed at 0.7 nA/V. The IETS shows (i) the low bias anomaly, (ii) several vibrational modes associated with $\nu$(C-S), $CH_2$ wag, and $\nu$(C-C) vibrations (50–200 meV), and (iii) the $\nu$(C-H) modes (~360–370 meV). Overall the agreement between theory and experiment is, in our opinion, good. Exceptions include (i) the size of the low bias anomaly, where we note that low frequency vibrations of the Au(111) substrate are not included in the calculations, and (ii) the amplitude of the C-H stretch peak, which will be discuss below. To study the details of the IETS we will in the remaining of this Letter focus on the C-H stretch mode region (200–400 meV) and the effects of deuteration.

Comparing the IETS of normal alkanethiol with methyl group deuterated alkanethiol, see Fig. 2, allows us to study the features of the IETS in detail. As expected, the isotope shifted $\nu$(C-D) signal, small peak at 255 meV and large peak at 273 meV, was only observed for $CD_3$-$C_7$, Fig. 2(b), and not for $CH_3$-$C_7$, Fig. 2(a). From a comparison with IR data [22] and our calculation, we assign the higher-energy peak with the larger intensity to be the asymmetric C-D stretching mode of the $CD_3$ [IR-$\nu_{as}(CD_3)$ 275 meV [22] and theory 278 meV] and the lower-energy peak with smaller intensity to the symmetric C-D stretching mode of the $CD_3$ [IR-$\nu_s(CD_3)$ 258 meV [22] and theory 256 meV]. The measured peak-area ratio of $\nu_{as}(CD_3)$ to $\nu_s(CD_3)$ was 80% to 20%. Comparison with the theoretical values of 84% and 16% underlines the quantitative agreement for the $CD_3$ modes. Additional measurements on shorter alkanethiol [$CD_3$-$(CH_2)_5$-S], not presented here, for different tip-sample distances shows that the $\nu(CD_3)$ IETS signal is stable and that the asymmetric mode is dominant even when a vacuum gap exists between the sample and the tip. The presence of the peaks of $\nu$(C-D) for $CD_3$-$C_7$ clearly demonstrates that the IETS detects the vibrations of the methyl group in contrast to the study by Beebe *et al.* [6]. They used a methyl group fluorinated alkanethiol molecule, and did not detect the $\nu(CF_3)$ mode directly or indirectly through intensity changes in the $\nu$(C-H) region. However, we find that the depletion of the $\nu$(C-H) peak area due to the methyl group deuteration is only 16%, which is smaller than their junction-to-junction IET signal variance (exceeded 20%) [6]. This makes it difficult to detect the relatively small intensity change in the $CH_3$ signal.

For macroscopic tunneling junctions (metal-insulator-molecule-metal), an empirical IETS selection rule has been suggested [23]. In these early IETS theories, tunneling electrons are assumed to interact with dynamic dipole moments via the long-range Coulomb force [24]. The strength of these dipole moments will be enhanced by

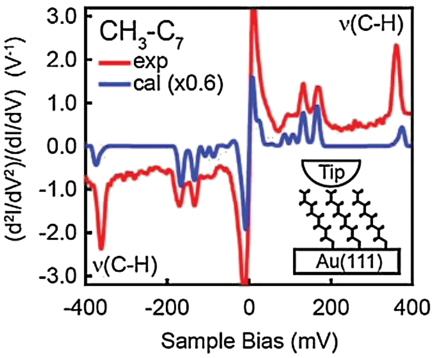

FIG. 1 (color). Comparison of experimental (red line) and calculated (blue line) inelastic electron tunneling spectroscopy (IETS) for $CH_3(CH_2)_7S$/Au(111) SAM ($CH_3$-$C_7$). The broadening in both experiment and theory is determined by the temperature (4.4 K) and the lock-in modulation voltage ($V_{mod}$ = 7.2 mV).

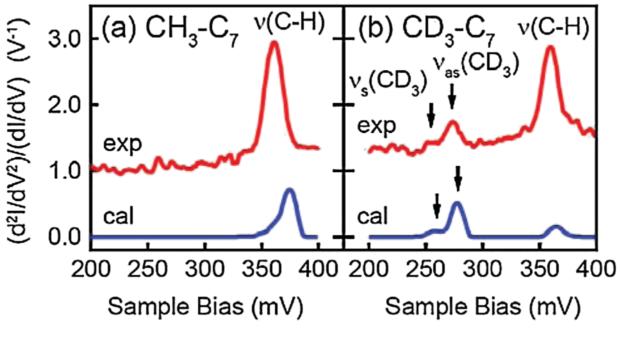

FIG. 2 (color). IETS for the C-D and C-H stretch region [$\nu$(C-D) and $\nu$(C-H)] for (a) $CH_3$-$C_7$ and (b) $CD_3$-$C_7$ SAMs on Au(111). The red lines and blue lines are the experimental and theoretical spectra, respectively ($V_{mod}$ = 7.2 mV).

image charges in the direction along the surface normal and reduced in the direction parallel to the surface. One can thus argue that the main IETS signal comes from dynamic dipole moments along the surface normal. Our measurements on the methyl group are inconsistent with this rule since the strong IETS signal comes from the asymmetric $CH_3$ stretch mode which has a much smaller dynamic dipole moment along the surface normal than the symmetric stretch [23].

Recently we proposed an approximate selection rule (propensity rule) based on the Fermi golden rule [16]:

$$I_{\text{inel}} \propto \sum_{n,m} |\langle \Psi_{\text{sn}}|\mathbf{M}|\Psi_{\text{tm}}\rangle|^2, \tag{1}$$

where $\Psi_{\text{sn}}$ are a set of scattering states incident from the substrate side, $\Psi_{\text{tm}}$ scattering states from the tip, and $\mathbf{M}$ is the $e$-ph coupling matrix. In our calculations we find that the IETS intensity is proportional to Eq. (1); e.g., the relative IETS weights of the asymmetric and symmetric $CD_3$ stretch mode are 84% to 16%, respectively. Unfortunately, the calculations do not provide a simple physical picture of why the asymmetric mode is more active because of (i) the large number of vibrational modes involved in the SAM and (ii) the large number of scattering states that need to be included. However, Eq. (1) does tell us that in order to get a large IETS signal, the $e$-ph coupling has to connect scattering states from the two leads. In other words, there is a connection between the IETS signal and the current path through the system [7].

We also see changes in the $\nu$(C-H) region for the deuterated molecule which can contribute to the assignment of the modes in the $\nu$(C-H) region. The blue lines and the red lines in Fig. 3(a) show the high-resolution IETS for $CH_3$-$C_7$ and $CD_3$-$C_7$, respectively. To compare the experimental spectra we use a smaller lock-in voltage ($V_{\text{mod}} = 2.7$ mV) and normalize their height. For the $CH_3$-$C_7$ (blue line), two peaks can be seen at the energies of 359 and 365 meV, while the curve for $CD_3$-$C_7$ (red curve) only shows a single peak whose energy coincides with that of the lower-energy component of the blue curve. The peak-area ratio of the low-energy component to the high-energy one was estimated, using Gaussians, to 5:1. Since the $\nu$(C-H) signal for the $CD_3$-$C_7$ molecule is expected to be derived only from the $CH_2$ group, we assign the components of 359 and 365 meV to the $CH_2$ and $CH_3$ groups, respectively. These assignments are consistent with IR measurements [25,26] where the $CH_2$ symmetric and asymmetric modes are at 354 and 362 meV, respectively. Comparison with our lower-energy $CH_2$ IETS peak centered at 359 meV indicates that the IETS intensity is given approximately equally by the asymmetric and symmetric $CH_2$ stretch modes. Additional measurements [17] on $CH_3(CH_2)_6CD_2S$ show, in contrast to the study by Beebe *et al.*, that the $\nu$(C-H) IETS intensity from the $CH_2$ groups close to the surface is 10%–20%; i.e., the linker part is not special in IETS. IR data further give the symmetric and asymmetric stretch mode of the $CH_3$ group [$\nu_s(CH_3)$ and $\nu_{\text{as}}(CH_3)$] at 360 [27] and 367 meV. These values are close to the low- and high-energy peaks of the IETS spectra and are consistent with the conclusion that the asymmetric mode is dominant for the methyl ($CH_3$) group. The experimental data therefore indicate that (i) the majority of the C-H stretch IETS signal originates from the $CH_2$ groups with (ii) approximately equal weights for $\nu_s(CH_2)$ and

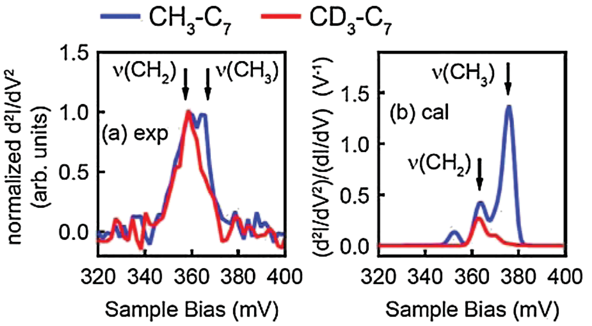

FIG. 3 (color). (a) Experimental and (b) theoretical high-resolution IETS around the $\nu$(C-H) modes for $CH_3$-$C_7$ (blue lines) and $CD_3$-$C_7$ (red lines) SAMs on Au(111) ($V_{\text{mod}} = 2.7$ mV). The experimental IETS intensity is normalized such that the peak height is unity for both cases.

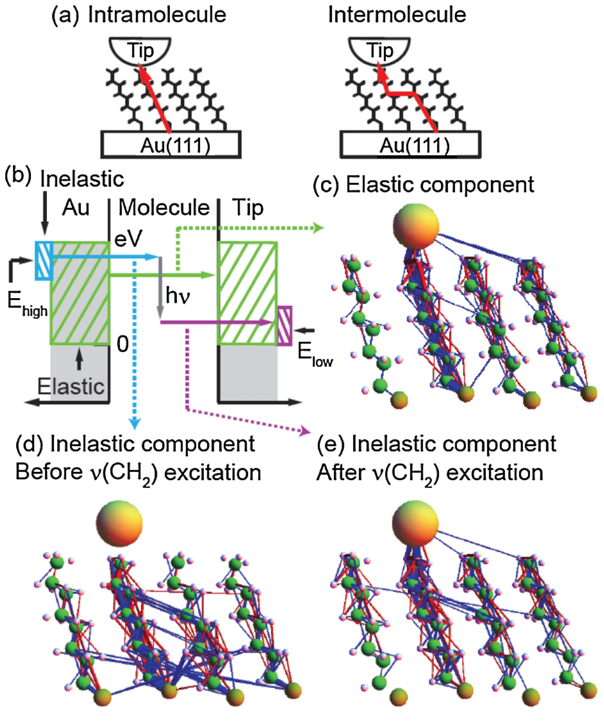

FIG. 4 (color). (a) Intramolecular and intermolecular current paths and (b) schematics of the energy-resolved elastic and inelastic processes. Current density plots (individually normalized) of the (c) elastic component and inelastic component (d) before and (e) after the $\nu(CH_2)$ excitation, where the cross-sectional area of the blue (red) cylinders is proportional to the current density and blue (red) indicates electrons flowing upwards (down). In the case of the inelastic process, the current density at $E_{\text{high}}$ (d) is continuously decreasing through the SAM due to emission of $\nu(CH_2)$ and scattering into $E_{\text{low}}$ (e).

$\nu_{as}(CH_2)$, (iii) a smaller ratio (1:5) from the $CH_3$ group of which (iv) the asymmetric $CH_3$ stretch dominates over the symmetric stretch mode.

The comparison with the theoretical calculations is less satisfying in the high-energy (~350–380 meV) range. The calculated vibrational energies are consistently 5–10 meV larger than the experimental data [$\nu_s(CH_3)$ 353, 365 meV, $\nu_{as}(CH_3)$ 375 meV, $\nu_s(CH_2)$ 363 meV, and $\nu_{as}(CH_2)$ 369 meV]. In addition, the IETS amplitude for the $\nu(CH_2)$ mode is severely underestimated; see Fig. 3(b). The quantitative agreement with experiments for the $\nu(CD_3)$ modes makes the poor performance for $\nu(CH_2)$ modes especially puzzling. However, it is also highly suggestive of the hypothesis that the discrepancy is due to inelastic intermolecular scattering, i.e., that the $\nu(CH_2)$ modes scatter electrons between the molecules of the SAM and/or that vibrations on nearby molecules influence the transport through the molecule under the tip; see Fig. 4(a). This idea can explain the poor agreement between theory and experiments since DFT is not well suited to describe intermolecular interactions. In addition, the magnitude of the $e$-ph coupling for the $\nu(CH_2)$ modes should be large between the molecules and could thus, according to Eq. (1), enable the intermolecular hopping. Our calculations, although giving a small IETS weight, indicate that intermolecular scattering is indeed important. As shown in Fig. 4(b), the main part of the current is carried by the elastic process, whose energy-resolved current density [17], assuming a positive tip bias, is shown in Fig. 4(c). Here, approximately 75% of the current travels through the molecule closest to the tip (second from the left in figures); i.e., the intramolecular tunneling [see Fig. 4(a)] is dominant in the elastic process. We have also studied the change in current densities due to inelastic scattering [only $\nu(CH_2)$ excitation considered here], where electrons start at $E_{\mathrm{high}}$ and end at $E_{\mathrm{low}}$ by exciting the vibration of $h\nu$ [see Fig. 4(b)]. The current density at $E_{\mathrm{high}}$ (before excitation) and $E_{\mathrm{low}}$ (after excitation) is shown in Figs. 4(d) and 4(e), respectively, where the former gradually decreases throughout the SAM as the electrons are scattered to $E_{\mathrm{low}}$. In the inelastic case, 62% of the current enters through the molecule closest to the tip. This is lower than the case of the elastic process and indicates that the electrons take a more intermolecular path than in the elastic process. In addition, Figs. 4(d) and 4(e) show a smaller part of the current entering the molecule under the tip [Fig. 4(d), second from the left] than exiting [Fig. 4(e)], which also indicates intermolecular scattering. Although this shows that intermolecular scattering is taking place in the DFT calculations, it is not a definite proof of the intermolecular scattering hypothesis and alternative explanations cannot be ruled out, e.g., supramolecular structures in the SAM. The reason for the theoretical underestimation of the $\nu(CH_2)$ IETS intensity must therefore be studied further.

In summary, we have investigated alkanethiol molecules using STM-based high-resolution inelastic electron tunneling spectroscopy (IETS). The fine resolution and partial deuteration of the molecule allowed us to identify and differentiate between methyl ($CH_3$) and methylene ($CH_2$) groups in addition to their symmetric and asymmetric C-H stretch modes. Comparison with first-principles calculations reveals quantitative agreement for the IETS originating from the methyl group including the approximately 4 times larger IETS signal for the asymmetric compared to the symmetric mode. However, the theory severely underestimates the contribution from the methylene groups. We also discuss the reason for this discrepancy and propose the hypothesis that intermolecular scattering may explain the difference.

We are deeply indebted to M. Yamashita, D. Kawakami, and T. Kajiwara for the synthesis of the methyl group deuterated alkanethiols. This research was partially supported by the Ministry of Education, Science, Sports and Culture, Grant-in-Aid for Scientific Research on Priority Areas, 448, 2005.

---

*komeda@tagen.tohoku.ac.jp

[1] H. B. Akkerman and B. de Boer, J. Phys. Condens. Matter **20**, 013001 (2008).
[2] M. A. Reed, Mater. Today **11**, 46 (2008).
[3] N. Okabayashi *et al.*, Phys. Rev. Lett. **100**, 217801 (2008).
[4] J. G. Kushmerick *et al.*, Nano Lett. **4**, 639 (2004).
[5] W. Y. Wang *et al.*, Nano Lett. **4**, 643 (2004).
[6] J. M. Beebe *et al.*, Nano Lett. **7**, 1364 (2007).
[7] A. Troisi and M. A. Ratner, Phys. Rev. B **72**, 033408 (2005).
[8] J. Jiang *et al.*, Nano Lett. **5**, 1551 (2005).
[9] Y. C. Chen *et al.*, Nano Lett. **5**, 621 (2005).
[10] G. C. Solomon *et al.*, J. Chem. Phys. **124**, 094704 (2006).
[11] M. Paulsson *et al.*, Nano Lett. **6**, 258 (2006).
[12] M. Paulsson *et al.*, Nano Lett. **9**, 117 (2009).
[13] N. Okabayashi and T. Komeda, Meas. Sci. Technol. **20**, 095602 (2009).
[14] Z. F. Li *et al.*, J. Agric. Food Chem. **53**, 3872 (2005).
[15] T. Frederiksen *et al.*, Phys. Rev. B **75**, 205413 (2007).
[16] M. Paulsson *et al.*, Phys. Rev. Lett. **100**, 226604 (2008).
[17] See supplementary material at http://link.aps.org/supplemental/10.1103/PhysRevLett.104.077801 for text and figures.
[18] P. Ordejón *et al.*, Phys. Rev. B **53**, R10 441 (1996).
[19] J. M. Soler *et al.*, J. Phys. Condens. Matter **14**, 2745 (2002).
[20] M. Brandbyge *et al.*, Phys. Rev. B **65**, 165401 (2002).
[21] L. J. Lauhon and W. Ho, Rev. Sci. Instrum. **72**, 216 (2001).
[22] E. Garand *et al.*, J. Phys. Chem. B **108**, 8182 (2004).
[23] *Tunneling Spectroscopy: Capabilities, Applications, and New Techniques*, edited by P. K. Hansma (Plenum, New York, 1982).
[24] D. J. Scalapino and S. M. Marcus, Phys. Rev. Lett. **18**, 459 (1967).
[25] R. G. Nuzzo *et al.*, J. Am. Chem. Soc. **112**, 558 (1990).
[26] S. C. Chang *et al.*, J. Am. Chem. Soc. **116**, 6792 (1994).
[27] Average of the two Fermi resonance peaks at 357 and 364 meV.